

PtNi nano-alloys loaded ordered mesoporous carbon for use in clofibric acid adsorption

S.E. Moradi^{a,*}, A. Nasrollahpour^a, J. Khodaveisi^b

^aYoung Researchers and Elite Club, Sari Branch, Islamic Azad University, Sari, Iran, Fax +98 11 33363168, email: er_moradi@hotmail.com (S.E. Moradi), a_nasrollahpour@hotmail.com (A. Nasrollahpour)

^bDepartment of Science, Sari Branch, Islamic Azad University, Sari, Iran

Received 7 January 2017; Accepted 3 August 2017

ABSTRACT

In this study, PtNi nano-alloys embedded in highly ordered mesoporous carbons have been prepared via an impregnation approach. The PtNi/OMC was characterized by BET surface area, TEM, XPS and XRD (low and wide angle) analysis. The adsorption of clofibric acid on PtNi/OMC with different variable such as: contact time, adsorbent dosage, initial concentration, pH, and temperature was investigated. The kinetic studies showed that the adsorption data followed a pseudo second-order kinetic model. The isotherm analysis indicated that the adsorption data can be represented by Langmuir isotherm model.

Keywords: Clofibric acid adsorption; Langmuir isotherm; Mesoporous carbon; Nickel; Platinum; Surface modification

1. Introduction

Nowadays, pharmaceuticals and personal care products (PPCPs) can be identified in municipal wastewater effluent (MWW) since wastewater treatment plants were not considered to eliminate PPCPs from their effluents. Consequently, many excesses of these compounds can be identified in both MWW and surface water bodies [1,2]. Moreover, pharmaceuticals possibly will also enter into human bodies because of the removal of agrochemicals, medical treatment or industrial by-products. It is also worth noting that veterinary-pharmaceuticals may reach surface and ground waters through manure [3]. In these concerns, clofibric acid (2-(4-chlorophenoxy)-2-methylpropanoic acid), the active metabolite of blood lipid regulators, is paid more attention by environmental scientists due to the large consumption of blood lipid regulators in terms of thousands of tons annually for therapeutic purposes suffering from angiocardopathy problem [4,5]. Clofibric acid has been frequently detected in wastewater treatment plant (WWTP) effluent, surface water, groundwater, and even drinking water. There are different procedures to remove PPCPs from water [6,7]. The most important treatment

procedures are coagulation [8], biodegradation [9,10], electrocoagulation [11], photo-transformation [12], chlorination [13], and ozonation [14]. A bibliographic revision reveals that adsorption has also been used as an alternative for the removal of clofibric acid from water [5,15–17]. The removal of pharmaceuticals by adsorption on commonly efficient adsorbents is one of the most promising techniques because of its convenience when applied in current water treatment processes [16,17]. To date, several reports related to the adsorption of pharmaceuticals onto natural materials or components of natural materials, e.g., soils [18], clays [19], graphene oxide [20], nanoporous carbon [21], and silica [22] have been published. To our knowledge, only few studies have been reported that address the removal of pharmaceuticals from aqueous media by nanoporous carbons, and in most of the cases, commercially available carbons were employed. Ordered mesoporous carbon (is a carbon based material containing ordered pores with diameters between 2 and 50 nm) is a good candidate removal of pharmaceuticals because of its high packing density, and good chemical stability, high specific surface area [23–25].

As mentioned, mesoporous carbon [21,22,26–28] have been used extensively in the adsorptive removal of hazardous materials. The adsorption phenomena entirely depend on the nature of the adsorbate and adsorbent. So

*Corresponding author.

far, a variety of interactions has been reported to describe the adsorption phenomena such as simple electrostatic interactions [29], π -complexation [30], acid-base interactions [31], H-bonding [32], metal complex formation [33], etc. In the case of PPCP adsorption, the most common phenomena is electrostatic interactions or metal complex formation with the adsorbents loaded with active metals like Ni, Pt, Cu, Co, etc. [34–37]. Researchers have reported employing single metal modified nanoporous materials for PPCP adsorption in aqueous solution [34–37], but no previous studies have reported the use of double metal modified mesoporous carbon for the adsorption of PPCPs from aqueous solutions. In this work, due to its high surface area, pore volume, accessible pore channel and simple pore chemistry, ordered mesoporous carbon derived from SBA-15 has been used as a model sorbent for the incorporation of active metals (platinum-nickel alloy) onto its surface in order to add or increase the adsorption capacity towards clofibric acid as target compound. The influence of different operational parameters such as contact time, initial concentration, adsorbent dose, pH, and temperature on clofibric acid adsorption by PtNi/OMC has been analyzed. Additionally, a kinetic modeling of the process has been performed and the experimental results have been fitted to two models, namely pseudo-first order, pseudo-second order models.

2. Experimental section

2.1. Materials

The reactants used in this study were Triblock copolymer Pluronic F127 (poly(ethylene oxide)-block-poly(propylene oxide)-block-poly-(ethylene oxide), PEO₁₀₆-PPO₇₀-PEO₁₀₆, MW = 12,600 Da), sucrose (C₁₂H₂₂O₁₁, 99%), sulfuric acid (H₂SO₄, 98%), ethanol absolute (C₂H₆O), citric acid (C₆H₈O₇), oxalic acid (H₂C₂O₄), nickel(II) chloride hexahydrate (NiCl₂·6H₂O), poly(vinyl pyrrolidone) (PVP, MW = 40,000), Sodium borohydride (NaBH₄), Potassium hexachloroplatinate (K₂PtCl₆), HCl (37%). The chemicals were used as received without any further purification. All chemicals were of analytical grade from Merck co (Merck, Darmstadt, Germany).

2.2.1. Mesoporous silica and unmodified mesoporous carbon samples

SBA-15 silica was prepared according to the procedure reported by Zhao et al. [38] by using a non-ionic oligomeric alkyl-ethylene oxide surfactant (Pluronic 127) as a structure directing agent, after that template was removed by means of calcinations at 500.0°C in flowing air. Ordered porous carbon was synthesized via a two-step impregnation of the mesoporous of SBA-15 with a solution of sucrose using an incipient wetness method [39]. Briefly, 1.0 g of the as-prepared SBA-15 was impregnated with an aqueous solution obtained by dissolving 1.1 g of sucrose and 0.14 g of H₂SO₄ in 5.0 g of deionized water. The mixture was then dried at 100.0°C for 6.0 h, and subsequently at 160.0°C for 6.0 h. The silica sample, containing partially polymerized and carbonized sucrose, was treated again at 100.0 and 160.0°C after the addition of 0.65 g of sucrose,

90 mg of H₂SO₄ and 5.0 g of deionized water. The sucrose-silica composite was then heated at 900.0°C for 4.0 h under nitrogen to complete the carbonization. The silica template was dissolved with 5.0 wt% hydrofluoric acid at room temperature. The template-free carbon product thus obtained was filtered, washed with deionized water and ethanol, and dried.

2.2. PtNi nanoalloys loaded ordered mesoporous carbon

In a typical synthesis, ordered mesoporous carbon (48 mg) were pretreated with 5 M HCl and concentrated HNO₃ solution before being suspended in 20.0 mL of deionized water. NiCl₂·6H₂O (11.3 mg) and poly(vinyl pyrrolidone) (PVP, MW = 40,000, 130 mg) are dissolved in 100.0 mL of ultra-pure H₂O (18.2 MW), sonicated for 30 min, and purged with Ar for 30.0 min. ordered mesoporous carbon supports were then added to the above solution, sonicated for 15.0 min. A freshly prepared solution of NaBH₄ (15 mg in 40.0 mL of H₂O) is then added dropwise under stirring. Immediately after all of the NaBH₄ has been added, K₂PtCl₆ (23.1 mg in 40.0 mL H₂O) (atomic ratio of Pt and Ni = 1:1) is added dropwise with stirring. After 30.0 min, the product is collected by centrifugation, washed several times with H₂O and ethanol, the obtained catalyst was dried in a vacuum oven at 70.0°C overnight, the PtNi/OMC nanocomposite were obtained.

2.3. Textural and structural studies

The morphology and surface structure of PtNi/OMC was examined by X-ray diffraction (XRD, Philips Xpert MPD, Eindhoven, The Netherlands) and The X-ray photoemission spectroscopy (XPS) analysis was acquired by using a Scienta ESCA 200 analyzer (Gammadata, Sweden) equipped with a monochromatized Al K α X-ray source. Transmission electron microscope (TEM) analysis was conducted with a JEM 2100 transmission electron microscope (JEOL, Japan) at 200 kV. The composition and thermal properties of PtNi/OMC were determined by TGA with a PL Thermal Sciences; model PL-STA (Thermal Sciences, UK) using a heating rate of 10°C/min from room temperature to 800.0°C under Ar. The measurements were conducted using approximately 3 mg samples and then weight retention/temperature curves were recorded.

Volumetric nitrogen sorption studies were taken at 77°K using a Micromeritics ASAP 2020 (Micromeritics Inc., USA) system. Before measurements, the samples were degassed below 1.33 Pa at 90.0°C for 1.0 h and heated (10°C/min) to 350.0°C for 10 h. The specific surface area (S_{BET}) was calculated by the BET method in the relative pressure range of 0.04–0.20. Total pore volume (V_{t}) was calculated at relative pressure $p/p = 0.98$. The microporous volume (V_{mi}) was determined by applying Dubinin–Radushkevich (DR) analyses on the corresponding isotherms in the relative pressure range 10^{-4} – 10^{-2} . The volume of pores smaller than 1 nm ($V < 1$ nm) was determined by the cumulative pore volume in the relative pressure range 10^{-6} – 10^{-4} using Horvath–Kawazoe (HK) method. The meso- and micropore sizes of samples were analyzed by the Barrett–Joyner–Halenda (BJH) [40] and HK methods, respectively.

2.4. Adsorption studies

A stock solution of 100 mg/L (pH of 6.0) of clofibric acid was prepared by dissolving an appropriate amount of the clofibric acid in ultra-pure water (18 MΩ cm) derived from a Milli-Q plus 185 water purifier (Millipore, Bedford, MA, USA). A pH meter (model 713, Metrohm, Herisau, Switzerland) with a combined glass electrode was used for pH measurements. 0.1 g PtNi/OMC adsorbent was added to 100.0 mL of clofibric acid solutions (10–50 mg/L) and the mixture was shaken on a rotary shaker at 150 rpm for different times. After adsorption, the suspension was centrifuged at 10,000 rpm for 10 min. The amount of clofibric acid adsorbed was calculated by subtracting the amount found in the supernatant liquid after adsorption from the amount of clofibric acid present before addition of the adsorbent by UV-Vis spectrophotometer (UV mini 1240 shimadzu, Shimadzu, Kyoto, Japan). Absorbance was measured at wavelength (λ_{\max}) 227 nm for determination of clofibric acid content. Calibration experiments were done separately before each set of measurements with clofibric acid solution of different concentrations. The effect of temperature on the adsorption of clofibric acid by PtNi/OMC was investigated by incubating the samples under different temperature conditions (303, 313, 323, and 333 K). To study the influence of pH on adsorption of clofibric acid by PtNi/OMC, the initial pH of PtNi/OMC was adjusted from 2.0 to 12.0 using NaOH or HCl aqueous solution. All tests were performed in triplicate to ensure reproducibility of the results; the mean of these measurements was taken to represent each evaluation. Calculations of amounts of adsorption of clofibric acid onto PtNi/OMC were based on adsorption capacity [Eqs. (1) and (2)].

$$q_e = \frac{(C_o - C_e) V}{W} \quad (1)$$

$$\text{Adsorption percent} = \frac{(C_o - C_e)}{C_o} * 100 \quad (2)$$

where q_e (mg/g) is equilibrium adsorption capacity, C_o and C_e (mg/L) are the initial and equilibrated clofibric acid concentrations, respectively. V (L) is the volume of solution and W (g) is the adsorbent mass.

2.5. Adsorption kinetics of clofibric acid

For sorption kinetics, a series of 250.0 mL flask containing 0.1 g of PtNi/OMC and 100.0 mL of clofibric acid solution at concentration 100 mg/L (pH of 6.0) was prepared. The mixtures were continuously shaken at 303°K and 150 rpm. Samples were taken at different time intervals and centrifuged at 10,000 rpm for 10 min and the upper solution were analyzed for clofibric acid concentration. The adsorption capacity (q_t , mg/g) at any time, it was calculated using the following equation:

$$q_t = \frac{(C_o - C_t) V}{W} \quad (3)$$

where C_t (mg/L) is the clofibric acid concentrations at time t .

2.6. Reproducibility and accuracy of the results

All batch isotherm experiments were simulated three times to establish accuracy, reliability and reproducibility. All glassware was presoaked in a 5% HNO₃ solution, rinsed with deionized water and oven-dried. Blanks were run and corrections applied, if necessary. Each batch adsorption experiment was conducted triplicate and the data shown are the average values. The individual values were generally within 5%.

3. Results and discussion

3.1. Textural characterization

Nitrogen physisorption is the method of choice to gain knowledge about mesoporous materials. This method gives information on the specific surface area and the pore diameter. Calculating pore diameters of mesoporous materials using the BJH method [41] is common. Former studies show that the application of the BJH theory gives appropriate qualitative results which allow a direct comparison of relative changes between different mesoporous materials.

As shown in Fig. 1, OMC and PtNi/OMC samples show type IV isotherms with obvious hysteresis loops, indicating that OMC samples are typical mesoporous materials. It also can be seen from the inset of Fig. 1 that the pore sizes of OMC and PtNi/OMC locate in mesopore size range and their most probable pore diameter are 3.7 and 3.5 nm, respectively. From the nitrogen sorption isotherms, it can be seen that the obtained nickel platinum alloy loaded carbons still have type IV isotherm, indicating that mesoporosity is preserved. The textural parameters listed in Table 1 clearly confirm the structure PtNi/OMC.

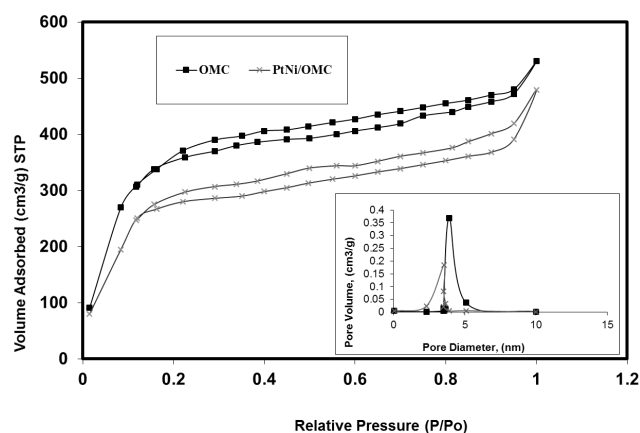


Fig. 1. Adsorption-desorption isotherms of nitrogen at 77K on OMC and PtNi/OMC. The insert shows the BJH pore size distribution calculated from the desorption branch of the isotherm.

Table 1
The surface area and porosity of OMC and PtNi/OMC samples

Sample	BET surface area (m ² /g)	Pore volume (cm ³ /g)
OMC	2544	0.99
PtNi/OMC	1768	0.84

Fig. 2 reports low angle XRD patterns of OMC and PtNi/OMC. With both samples, the main reflection peak is well preserved, representing that rather ordered mesoporous materials with hexagonal structures were obtained.

The wide-angle XRD patterns of PtNi/OMC in Fig. 3 exhibit two resolved diffraction peaks at 44.6° (111) and 51.9° (200) 2θ , characteristic of metallic nickel with a FCC structure. Moreover, the diffraction peaks at 49.1° , 56.2° , 81.3° and 99.7° can be assigned to reflections from the (111), (200), (220) and (311) planes of the face-centered-cubic Pt, indicating a good crystallinity of the supported nanoparticles. It reveals that both the nickel and the platinum species in the mesoporous carbon matrix exists in metallic form.

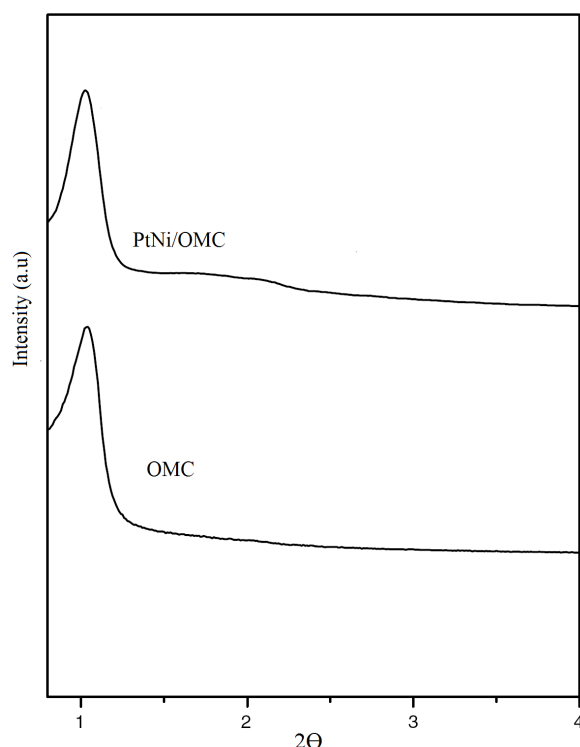


Fig. 2. Low angle XRD patterns of OMC and PtNi/OMC adsorbents.

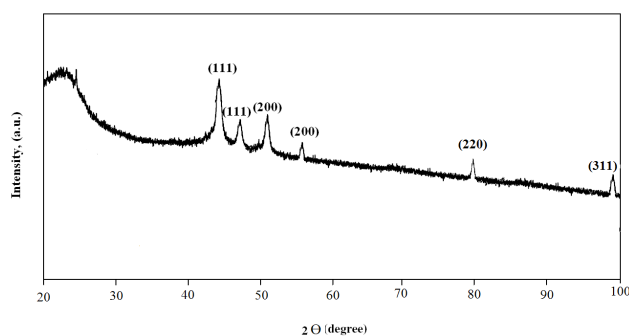


Fig. 3. The wide angle XRD patterns of PtNi/OMC adsorbent.

Representative TEM image of the obtained PtNi/OMC is shown in Fig. 4a. The TEM image (Fig. 4a) of PtNi/OMC also show that platinum-nickel nanoparticles are relatively well-dispersed on the ordered mesoporous carbon surface. The mean size of PtNi/OMC calculated from the TEM image is around 11.0 nm. The histogram of particle size for PtNi/OMC show that the size distribution is relatively narrow (Fig. 4b).

Fig. 5 displays Pt 4f and Ni 2p X-ray photoelectron spectroscopy (XPS) spectra of PtNi/OMC composites. The two characteristic peaks at 71.3 eV (Pt 4f_{7/2}) and 74.5 eV (Pt 4f_{5/2}) are observed in Fig. 5a, confirming the formation of metallic Pt. The Ni 2p peaks (Fig. 5b) were curve fitted into 852.6 eV for Ni 2p_{3/2}, indicating the existence of Ni. The Ni⁰ state is a reflection of metallic Ni decomposed from the Ni precursor.

3.2. Adsorption studies

3.2.1. Effect of contact time and initial concentration

Experiments were directed for different time intervals to determine duration required to reach adsorption equilibrium. Experiments showed that the amount of adsorbed clofibric acid progressively increased with the rise of contact time. As follows from Fig. 6, the resultant equilibrium time amounts to 180 min.

Clofibric acid solutions at different initial concentration (10, 20, 50 mg/L) were treated with 1.0 g/L of PtNi/OMC. Fig. 6 shows the effect of varying clofibric acid concentrations against the amount of clofibric acid adsorbed. The amount of clofibric acid equilibrium adsorption removal increases with an increase in initial solution concentration from 13.3 to 46.5 mg/g for PtNi/OMC. This is because of the fact that by increasing the concentration of clofibric acid in solution the availability of clofibric acid at the adsorbent interface also increases. When the surface active sites of adsorbent are covered fully, the extent of adsorption reaches a limit resulting in saturated adsorption.

3.2.2. Effect of adsorbent dose

Adsorbent dosage is an essential factor influencing adsorption processes meanwhile it determines the adsorption capacity of an adsorbent for a given initial concentration of the adsorbate at the operating conditions. The effect of PtNi/OMC on removal of clofibric acid was studied in range of 0.5–20 g/L. Fig. 7 exhibited that despite the adsorption capacity of sorbent removal percent increased, as adsorbent dosage increased from 0.5 to 1 g/L. It is ascribed to an increase in the adsorptive surface area and the availability of more binding sites. At higher adsorbent dosages significant increase in removal percent of clofibric acid is not happening. Consequently, 1 g/L adsorbent dosage was chosen as optimum dosage for further analysis.

3.2.3. Effect of solution pH on clofibric acid adsorption capacity

pH is an important factor in controlling the adsorption of pollutant onto adsorbent, which affects the surface charge of the adsorbent and the degree of ionization of the

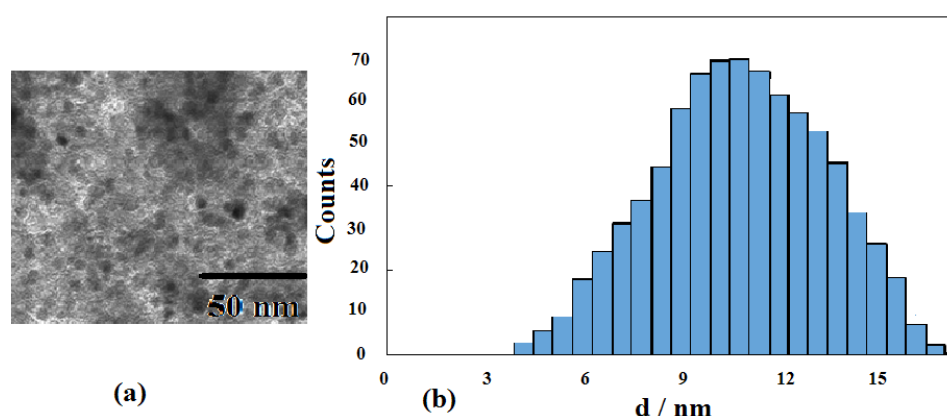


Fig. 4. (a) TEM photographs and (b) histogram of particle size distribution of PtNi/OMC adsorbent.

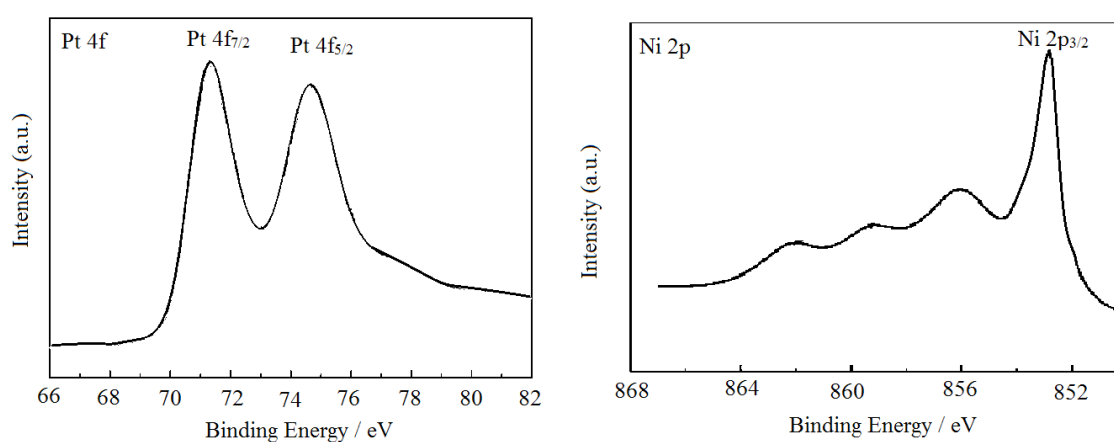


Fig. 5. (a) XPS spectra of Pt 4f in the PtNi/OMC composites and (b) XPS spectra of Ni2p in the PtNi/OMC composites.

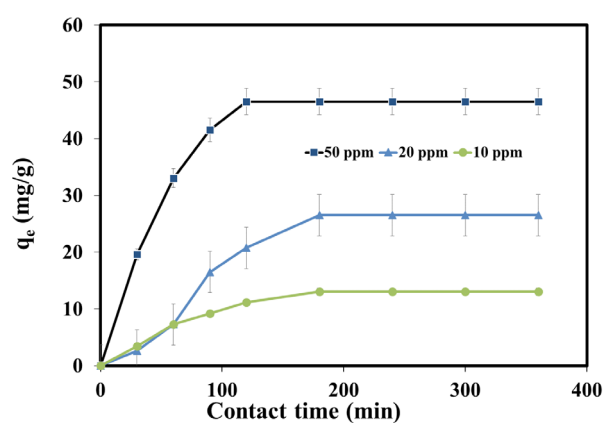


Fig. 6. Effect of contact time and initial concentration on removal of clofibric acid by PtNi/OMC (agitation speed = 150 (rpm), adsorbent dosage = 0.5 g/L, temperature = 303 K, pH = 6.0).

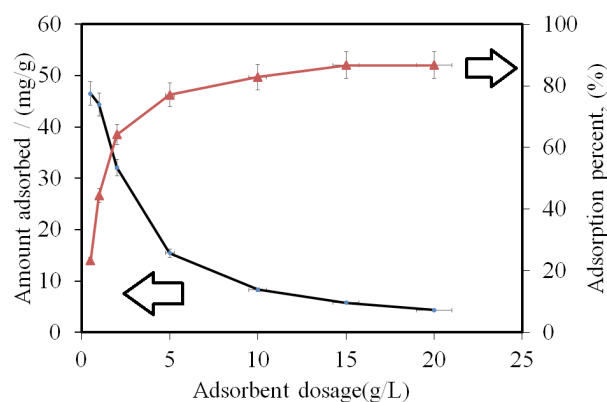


Fig. 7. Effect of PtNi/OMC adsorbent dosage on the adsorption of clofibric acid. ([clofibric acid] = 100 mg/L, agitation speed = 150 (rpm), contact time = 3.0 h, temperature = 303 K, pH = 6.0).

adsorbate. In order to find out the effect of pH, 10.0 mg of the OMC the and PtNi/OMC sorbents were treated separately with 50.0 mL of 100 mg/L clofibric acid at various pH values (from 2.0 to 12.0) accompanied by mild shaking

at room temperature for 3.0 h. Fig. 8 shows the effect of pH on adsorption of clofibric acid by PtNi/OMC. It was found that the adsorption capacity of clofibric acid increased with increasing the solution pH up to pH of 6.0. This could be

attributed to the fact that the protonation of carbonyl and hydroxyl groups of clofibric acid became insignificant at high pH. Under these domain of pH, non-electrostatic interactions are responsible for the interaction between clofibric acid and the surface of mesoporous carbon. At relative high range of pH values, the reduced protons corresponding to the increased negative active sites on OMC adsorbent promotes the electrostatic and H-bonding interactions with clofibric acid functional groups. At high pHs, clofibric acid is negatively charged whereas the surface of OMC shows a progressively more negative charge. This leads to an electrostatic repulsion between the solute and the adsorbent. But, OMC can form a strong π - π interaction with clofibric acid because of the large delocalized π -electron system of ordered mesoporous carbon. At very low and very high pH good adsorption for clofibric acid has been shown, it because of the fact that the π - π interaction is not depend on pH of solution.

3.2.4. Adsorption kinetics

The kinetic data was fitted with two commonly used pseudo-first-order and pseudo-second-order models to obtain the rate of the reaction and their linear forms are represented as given below:

$$\log (q_e - q_t) = \log q_e - \frac{k_1 t}{2.303} \quad (4)$$

$$\frac{t}{q_t} = \frac{1}{k_2 q_e^2} + \frac{t}{q_e} \quad (5)$$

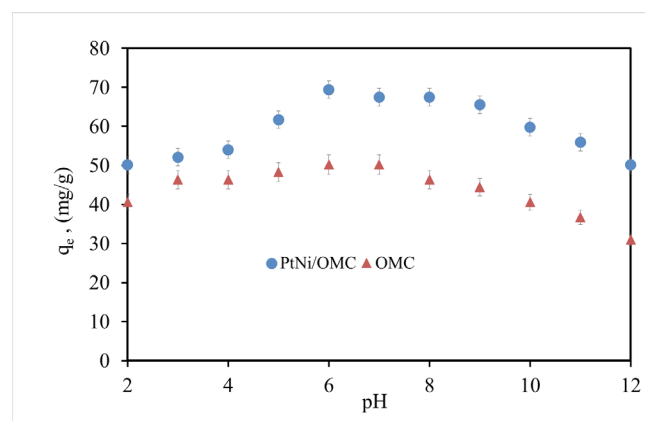


Fig. 8. Adsorption of clofibric acid on OMC and PtNi/OMC as a function of pH (adsorbent dosage = 1 g/L, [clofibric acid] = 100 mg/L, agitation speed = 150 (rpm), temperature = 303 K).

Table 2

Parameter values of the kinetics models fitting to the experimental results for clofibric acid by OMC and PtNi/OMC ([clofibric acid] = 50 ppm, agitation speed = 150 (rpm), adsorbent dosage = 1 g/L, temperature = 303 K, pH = 6)

Adsorbent	Pseudo-first order model			Pseudo-second order model		
	k_1 (L/min)	R^2	q_e (mg/g)	k_2 (g/mg.min)	R^2	q_e (mg/g)
OMC	0.008	0.9657	19.7	1.6×10^{-5}	0.9968	22.9
PtNi/OMC	0.011	0.9722	35.8	2.2×10^{-5}	0.9953	36.1

where k_1 (L/min) and k_2 (g/mg.min) are the pseudo-first-order and pseudo-second-order rate constants, respectively. The kinetic adsorption data were fitted to Eq. (4) and Eq. (5), and the calculated results are listed in Table 2. The correlation coefficients (R^2) for pseudo-second-order model are all higher than for pseudo-first-order model and the experimental data fit to the pseudo-second-order model better than pseudo-first-order model. The results indicate that chemical adsorption might be the rate-limiting step. From the pseudo-first-order and pseudo-second-order models, the rate of clofibric acid adsorption on PtNi/OMC was determined to be 0.011 L/min and 2.2×10^{-5} g/mg.min and the predicted q_e values were 35.8 and 36.1 mg/g, respectively (Table 2).

3.2.5. Adsorption thermodynamics

The adsorption isotherm of clofibric acid on PtNi/OMC at four different temperatures (303–333 K) was investigated. It has shown that the adsorption of clofibric acid on PtNi/OMC is promoted at higher temperatures. Thermodynamic parameter related to the adsorption process, i.e., free energy change (ΔG , kJ/mol) for adsorption clofibric acid on PtNi/OMC was calculated using Eq. (6).

$$\Delta G = -RT \ln (55.5 K_L) \quad (6)$$

where R is the universal gas constant (8.314 J/mol.K), T is the temperature and K_L is Langmuir constant (L/mol) obtained from the plot of C_e/q_e vs. C_e . The calculated ΔG value was found to be -18.3 to -21.0 kJ/mol. The negative value of free energy change indicated the spontaneous nature of sorption and confirmed affinity of mesoporous carbon adsorbents for the clofibric acid removal from water.

The enthalpy change ΔH and ΔS can be obtained from the van't Hoff equation, Eq. (7)

$$\ln K_L = \Delta S_R - \Delta H_R \times (1/T) \quad (7)$$

A linear plot of $\ln K_L$ vs. $1/T$ is obtained from the model. The enthalpy change (ΔH) and entropy change (ΔS) can be calculated from the slope and intercept of the van't Hoff plot, respectively. As shown in Table 3, the positive enthalpy change (ΔH) suggests that the adsorption of this work is an endothermic reaction.

3.2.6. Adsorption isotherms

Equilibrium adsorption isotherm is the one of the most essential design parameter expresses how the adsorbate

Table 3

Thermodynamic parameters for adsorption of clofibrac acid on OMC and PtNi/OMC ([clofibrac acid] = 50 ppm, agitation speed = 150 (rpm), adsorbent dosage = 1 g/L, temperature = 303–333 K, pH=6)

T(K)	C_e (mg/L)	q_e (mg/g)	K_c	ΔG° (kJ/mol)	ΔH° (kJ/mol)	ΔS° (J/ mol.K)
303	12.6	36.2	26.5	-18.3	94.2	280.3
313	11.4	37.4	30.01	-19.2		
323	10.6	38.2	32.77	-20.1		
333	9.7	39.1	36.32	-21.0		

interacts with the adsorbent. The sorption mechanism and affinity of the adsorbent could be clarified by modeling of isotherms by different equilibrium models [34]. In this study, the two most common isotherms, Langmuir and Freundlich models, were used to describe the experimental adsorption data. Langmuir model assumes monolayer adsorption onto a surface which consists of finite number of active sites having a uniform energy. The linear form of Langmuir isotherm equation is given as Eq. (8).

$$\frac{C_e}{q_e} = \frac{C_e}{Q_o} + \frac{1}{(Q_o \times b)} \quad (8)$$

where, C_e (mg/L) is equilibrium concentration of adsorbate; q_e (mg/g) is the amount of adsorbate adsorbed; Q_o (mg/g) is Langmuir constant (maximum adsorption capacity); b (L/mg) is Langmuir constant.

According to Freundlich model, it was often applicable to describe the models of multilayer adsorption onto the surface of heterogeneous sites with different bond energy. The equation of Freundlich model is given as follows:

$$\log q_e = \log K_F + \frac{1}{n} \log C_e \quad (9)$$

where q_e is the amount and the maximum amount of adsorbed phosphate per unit weight of adsorbent (mg/g), respectively, C_e is the residual concentration of adsorbate in bulk solution (mg/L), K_L is a constant determined by plotting C_e/q_e vs. C_e , K_F and $1/n$ are the constants related to adsorption of adsorbent and intensity of the adsorption, respectively.

These two Models fit to equilibrium adsorption results of clofibrac acid on PtNi/OMC were assessed based on the values of the determination coefficient (R^2) of the linear regression plot. The obtained experimental data were fit with these two models. The Langmuir and Freundlich isotherms were found to be linear over the whole concentration range studied with higher R^2 values (>0.99) In addition, the Langmuir and Freundlich model parameters for the adsorption of clofibrac acid on PtNi/OMC adsorbents are listed in Table 4. The maximum monolayer capacities of clofibrac acid, q_{max} , obtained from Langmuir model are 27.4 and 38.5 mg/g for OMC and PtNi/OMC, respectively. It was important that the maximum adsorption capacity of the PtNi/OMC is much larger than that of pristine OMC and comparable with other adsorbents [5,15–17]. The higher

Table 4

Langmuir and Freundlich constants for adsorption clofibrac acid removal on OMC and PtNi/MC

Adsorbent	Langmuir			Freundlich		
	q_m (mg/g)	b (L/mg)	R^2	K_F (mg/g)	n (L/mg)	R^2
OMC	27.4	0.0121	0.9991	15.4	2.7	0.9864
PtNi/MC	38.5	0.0095	0.9997	37.6	4.4	0.9752

adsorption capacity of PtNi/OMC can be explained by several facts. Undoubtedly, increasing in chemical (complexation between platinum and nickel nanoparticles located on PtNi/OMC and clofibrac acid, as proven by XPS and XRD examinations) as a cause of presence of platinum and nickel nanoparticle in PtNi/OMC.

The critical features of the Langmuir isotherm can be expressed by a dimensionless constant separation factor R_L given by following relation that can be used to determine the possibility of adsorption in a specified concentration range over adsorbents Eq. (10).

$$R_L = \frac{1}{1 + bC_o} \quad (10)$$

The calculated R_L values at different initial clofibrac acid concentration were in the range of 0.021–0.054, which lie between 0 and 1, confirming that the adsorption of clofibrac acid on PtNi/OMC was favorable.

4. Conclusion

Adsorption of clofibrac acid onto OMC and PtNi/OMC was performed to find the optimum conditions. The consequences of experiments presented that at pH of 6.0, an amount of adsorbent of 1 g/L and a time of 3.0 h were optimal conditions for the removal of 50 mg/L of clofibrac acid. The pseudo-second-order kinetic model best described the adsorption behavior of clofibrac acid onto PtNi/OMC. PtNi/OMC exhibited good kinetic characteristics (equilibrium time 3.0 h) and high adsorption capacity for clofibrac acid. Equilibrium adsorption isotherm was fitted well with Langmuir model.

Acknowledgments

The authors thank The Research Council at the Azad University for financial support.

References

- [1] A. Hu, X. Zhang, D. Luong, K.D. Oakes, M.R. Servos, R. Liang, S. Kurdi, P. Peng, Y. Zhou, Adsorption and photocatalytic degradation kinetics of pharmaceuticals by TiO₂ nanowires during water treatment, *Waste Biomass Valor*, 3 (2012) 443–449.
- [2] B.D. Blair, J.P. Crago, C.J. Hedman, R.D. Klaper, Pharmaceuticals and personal care products found in the Great Lakes above concentrations of environmental concern, *Chemosphere*, 93 (2013) 2116–2123.
- [3] S.K. Khetan, T.J. Collins, Human pharmaceuticals in the aquatic environment: A challenge to green chemistry, *Chem. Rev.* (Washington, DC, U. S.), 107 (2007) 2319–2364.

- [4] W. Li, S. Lu, Z. Qiu, K. Lin, UV and VUV photolysis vs. UV/H₂O₂ and VUV/H₂O₂ treatment for removal of clofibric acid from aqueous solution, *Environ. Technol.*, 32 (2011) 1063–1071.
- [5] Y. Nie, S. Deng, B. Wang, J. Huang, G. Yu, Removal of clofibric acid from aqueous solution by polyethylenimine-modified chitosan beads, *Front. Environ. Sci. En.*, 8 (2014) 675–682.
- [6] B.T. Ferrari, N. Paxéus, R.L. Giudice, A. Pollio, J. Garric, Ecotoxicological impact of pharmaceuticals found in treated wastewaters: study of carbamazepine, clofibric acid, and diclofenac, *Ecotoxicol. Environ. Saf.*, 55 (2003) 359–370.
- [7] C. Tixier, H.P. Singer, S. Oellers, S.R. Müller, Occurrence and fate of carbamazepine, clofibric acid, diclofenac, ibuprofen, ketoprofen, and naproxen in surface waters, *Environ. Sci. Technol.*, 37 (2003) 1061–1068.
- [8] K.-J. Choi, S.-G. Kim, S.-H. Kim, Removal of antibiotics by coagulation and granular activated carbon filtration, *J. Hazard. Mater.*, 151 (2008) 38–43.
- [9] K. Onesios, J. Yu, E. Bouwer, Biodegradation and removal of pharmaceuticals and personal care products in treatment systems: a review, *Biodegradation*, 20 (2009) 441–466.
- [10] A. Joss, S. Zabczynski, A. Göbel, B. Hoffmann, D. Löffler, C.S. McArdell, T.A. Ternes, A. Thomsen, H. Siegrist, Biological degradation of pharmaceuticals in municipal wastewater treatment: Proposing a classification scheme, *Water Res.*, 40 (2006) 1686–1696.
- [11] M. Boroski, A.C. Rodrigues, J.C. Garcia, L.C. Sampaio, J. Nozaki, N. Hioka, Combined electrocoagulation and TiO₂ photoassisted treatment applied to wastewater effluents from pharmaceutical and cosmetic industries, *J. Hazard. Mater.*, 162 (2009) 448–454.
- [12] S. Canonica, L. Meunier, U. von Gunten, Phototransformation of selected pharmaceuticals during UV treatment of drinking water, *Water Res.*, 42 (2008) 121–128.
- [13] D. Simazaki, J. Fujiwara, S. Manabe, M. Matsuda, M. Asami, S. Kunikane, Removal of selected pharmaceuticals by chlorination, coagulation–sedimentation and powdered activated carbon treatment, *Water Sci. Technol.*, 58 (2008).
- [14] Q. Sui, J. Huang, S. Lu, S. Deng, B. Wang, W. Zhao, Z. Qiu, G. Yu, Removal of pharmaceutical and personal care products by sequential ultraviolet and ozonation process in a full-scale wastewater treatment plant, *Front. Environ. Sci. Eng.*, 8 (2014) 62–68.
- [15] C.-M. Dai, J. Zhang, Y.-I. Zhang, X.-F. Zhou, Y.-P. Duan, S.-G. Liu, Removal of carbamazepine and clofibric acid from water using double templates–molecularly imprinted polymers, *Environ. Sci. Pollut. R.*, 20 (2013) 5492–5501.
- [16] A.S. Mestre, A. Nabico, P.L. Figueiredo, M.L. Pinto, M.S.C.S. Santos, I.M. Fonseca, Enhanced clofibric acid removal by activated carbons: Water hardness as a key parameter, *Chem. Eng. J.*, 286 (2016) 538–548.
- [17] Z. Hasan, J. Jeon, S.H. Jhung, Adsorptive removal of naproxen and clofibric acid from water using metal-organic frameworks, *J. Hazard. Mater.*, 209 (2012) 151–157.
- [18] K.M. Onesios-Barry, D. Berry, J.B. Proescher, I.K.A. Sivakumar, E.J. Bouwer, Removal of pharmaceuticals and personal care products during water recycling: microbial community structure and effects of substrate concentration, *Appl. Environ. Microbiol.*, 80 (2014) 2440–2450.
- [19] K. Styszko, K. Nosek, M. Motak, K. Bester, Preliminary selection of clay minerals for the removal of pharmaceuticals, bisphenol A and triclosan in acidic and neutral aqueous solutions, *C. R. Chim.*, 18 (2015) 1134–1142.
- [20] Y.-L. Zhang, Y.-J. Liu, C.-M. Dai, X.-F. Zhou, S.-G. Liu, Adsorption of clofibric acid from aqueous solution by graphene oxide and the effect of environmental factors, *Water Air Soil Pollut.*, 225 (2014) 2064.
- [21] L. Ji, F. Liu, Z. Xu, S. Zheng, D. Zhu, Adsorption of pharmaceutical antibiotics on template-synthesized ordered micro- and mesoporous carbons, *Environ. Sci. Technol.*, 44 (2010) 3116–3122.
- [22] N. Suriyanon, J. Permrungruang, J. Kaosaiphun, A. Wongrueng, C. Ngamcharussrivichai, P. Punyapalakul, Selective adsorption mechanisms of antilipidemic and non-steroidal anti-inflammatory drug residues on functionalized silica-based porous materials in a mixed solute, *Chemosphere*, 136 (2015) 222–231.
- [23] K. Xia, Q. Gao, C. Wu, S. Song, M. Ruan, Activation, characterization and hydrogen storage properties of the mesoporous carbon CMK-3, *Carbon*, 45 (2007) 1989–1996.
- [24] C.-C. Huang, Y.-H. Li, Y.-W. Wang, C.-H. Chen, Hydrogen storage in cobalt-embedded ordered mesoporous carbon, *Int. J. Hydrogen Energy*, 38 (2013) 3994–4002.
- [25] S.E. Moradi, S. Amirmahmoodi, M.J. Baniamerian, Hydrogen adsorption in metal-doped highly ordered mesoporous carbon molecular sieve, *J. Alloys Compd.*, 498 (2010) 168–171.
- [26] M.J. Baniamerian, S.E. Moradi, A. Noori, H. Salahi, The effect of surface modification on heavy metal ion removal from water by carbon nanoporous adsorbent, *Appl. Surf. Sci.*, 256 (2009) 1347–1354.
- [27] X. Peng, F. Hu, F.L.Y. Lam, Y. Wang, Z. Liu, H. Dai, Adsorption behavior and mechanisms of ciprofloxacin from aqueous solution by ordered mesoporous carbon and bamboo-based carbon, *J. Colloid Interface Sci.*, 460 (2015) 349–360.
- [28] X. Peng, F. Hu, J. Huang, Y. Wang, H. Dai, Z. Liu, Preparation of a graphitic ordered mesoporous carbon and its application in sorption of ciprofloxacin: Kinetics, isotherm, adsorption mechanisms studies, *Microporous Mesoporous Mater.*, 228 (2016) 196–206.
- [29] K. Pillay, E.M. Cukrowska, N.J. Coville, Multi-walled carbon nanotubes as adsorbents for the removal of parts per billion levels of hexavalent chromium from aqueous solution, *J. Hazard. Mater.*, 166 (2009) 1067–1075.
- [30] Y. Li, Q. Du, T. Liu, X. Peng, J. Wang, J. Sun, Y. Wang, S. Wu, Z. Wang, Y. Xia, L. Xia, Comparative study of methylene blue dye adsorption onto activated carbon, graphene oxide, and carbon nanotubes, *Chem. Eng. Res. Des.*, 91 (2013) 361–368.
- [31] Y. Deng, C.M. Ezyske, Sulfate radical-advanced oxidation process (SR-AOP) for simultaneous removal of refractory organic contaminants and ammonia in landfill leachate, *Water Res.*, 45 (2011) 6189–6194.
- [32] H. Hou, R. Zhou, P. Wu, L. Wu, Removal of Congo red dye from aqueous solution with hydroxyapatite/chitosan composite, *Chem. Eng. J.*, 211–212 (2012) 336–342.
- [33] J. Gardiner, The chemistry of cadmium in natural water—II. The adsorption of cadmium on river muds and naturally occurring solids, *Water Res.*, 8 (1974) 157–164.
- [34] L. Wei, G. Yang, R. Wang, W. Ma, Selective adsorption and separation of chromium (VI) on the magnetic iron–nickel oxide from waste nickel liquid, *J. Hazard. Mater.*, 164 (2009) 1159–1163.
- [35] B. Cheng, Y. Le, W. Cai, J. Yu, Synthesis of hierarchical Ni(OH)₂ and NiO nanosheets and their adsorption kinetics and isotherms to Congo red in water, *J. Hazard. Mater.*, 185 (2011) 889–897.
- [36] M. Salimian, M. Ivanov, F.L. Deepak, D.Y. Petrovykh, I. Bdkin, M. Ferro, A. Kholkin, E. Titus, G. Goncalves, Synthesis and characterization of reduced graphene oxide/spiky nickel nanocomposite for nanoelectronic applications, *J. Mater. Chem. C*, 3 (2015) 11516–11523.
- [37] X. Yao, S. Deng, R. Wu, S. Hong, B. Wang, J. Huang, Y. Wang, G. Yu, Highly efficient removal of hexavalent chromium from electroplating wastewater using aminated wheat straw, *RSC Advances*, 6 (2016) 8797–8805.
- [38] D. Zhao, J. Sun, Q. Li, G.D. Stucky, Morphological control of highly ordered mesoporous silica SBA-15, *Chem. Mater.*, 12 (2000) 275–279.
- [39] S. Jun, S.H. Joo, R. Ryoo, M. Kruk, M. Jaroniec, Z. Liu, T. Ohsuna, O. Terasaki, Synthesis of new, nanoporous carbon with hexagonally ordered mesostructure, *J. Am. Chem. Soc.*, 122 (2000) 10712–10713.
- [40] E.P. Barrett, L.G. Joyner, P.P. Halenda, The determination of pore volume and area distributions in porous substances. I. Computations from nitrogen isotherms, *J. Am. Chem. Soc.*, 73 (1951) 373–380.
- [41] M.F. De Lange, T.J.H. Vlucht, J. Gascon, F. Kapteijn, Adsorptive characterization of porous solids: Error analysis guides the way, *Micropor. Mesopor. Mater.*, 200 (2014) 199–215.